NASA/TM—1998-208408

98–GT–285

Aerodynamics of a Transitioning Turbine Stator Over a Range of Reynolds Numbers

R.J. Boyle, B.L. Lucci, V.G. Verhoff, W.P. Camperchioli, and H. La
Lewis Research Center, Cleveland, Ohio

Prepared for the
Turbo Expo '98
sponsored by the American Society of Mechanical Engineers
Stockholm, Sweden, June 2–5, 1998

National Aeronautics and
Space Administration

Lewis Research Center

June 1998

Available from

NASA Center for Aerospace Information
7121 Standard Drive
Hanover, MD 21076
Price Code: A03

National Technical Information Service
5287 Port Royal Road
Springfield, VA 22100
Price Code: A03

AERODYNAMICS OF A TRANSITIONING TURBINE STATOR OVER A RANGE OF REYNOLDS NUMBERS

R. J. Boyle
B. L. Lucci
V. G. Verhoff
W. P. Camperchioli
H. La

NASA Lewis Research Center
Cleveland, OH 44135

ABSTRACT

Midspan aerodynamic measurements for a three vane-four passage linear turbine vane cascade are given. The vane axial chord was 4.45cm. Surface pressures and loss coefficients were measured at exit Mach numbers of 0.3, 0.7, and 0.9. Reynolds number was varied by a factor of six at the two highest Mach numbers, and by a factor of ten at the lowest Mach number. Measurements were made with and without a turbulence grid. Inlet turbulence intensities were less than 1% and greater than 10%. Length scales were also measured. Pressurized air fed the test section, and exited to a low pressure exhaust system. Maximum inlet pressure was two atmospheres. The minimum inlet pressure for an exit Mach number of 0.9 was one-third of an atmosphere, and at a Mach number of 0.3, the minimum pressure was half this value. The purpose of the test was to provide data for verification of turbine vane aerodynamic analyses, especially at low Reynolds numbers. Predictions obtained using a Navier-Stokes analysis with an algebraic turbulence model are also given.

Nomenclature

C_p	-	Surface pressure coefficient
C_τ	-	Constant in Autocorrelation fit
c	-	True chord
c_x	-	Axial chord
d	-	Grid tube diameter
$\bar{e}$	-	Kinetic energy loss coefficient
l	-	Distance from grid
M	-	Mach number
P	-	Pressure
R	-	Autocorrelation function
Re	-	Reynolds number
s	-	Surface distance
Tu	-	Turbulence intensity
U	-	Velocity
V	-	Voltage
x	-	Axial distance
Y	-	Total pressure loss coefficient
y	-	Pitchwise distance
α	-	Flow angle
Λ	-	Length scale
λ	-	Pressure gradient parameter
ρ	-	Density
τ	-	Time

Subscripts

A	-	Area averaged
M	-	Mass averaged
P	-	Pressure surface
S	-	Suction surface
1	-	Vane inlet
2	-	Vane exit

Superscripts

$'$	-	Total condition
$\bar{}$	-	Average

INTRODUCTION

Depending on the application, the Reynolds number for a gas turbine engine can be less than 1×10^5 to over 1×10^6. In addition to the size of the blades, the operating conditions of the engine result in large Reynolds number variations. Mayle (1991), and Hourmouziadis (1989) discuss the variation in Reynolds number for aircraft turbines with altitude and stage location. Thus, in a particular engine the blade Reynolds number may be more than a factor of five lower in the low pressure turbine than in the high pressure turbine. Also, between takeoff and cruise the blade Reynolds number decreases by about a factor of three. At the same inlet pressure and temperature, a gas turbine with an output of 5000 hp will have a blade Reynolds number approximately one-third of that for a 50,000 hp turbine.

To accurately predict aerodynamic and heat transfer characteristics of a turbine blade row it is necessary to understand the influences of various parameters on the blade row performance. Among these parameters are Reynolds and Mach numbers, turbulence intensity and scale, surface pressure distribution, as well as upstream blade passing frequency. The principal effect of variations in these parameters in the aerodynamics and heat transfer is to change the location of transition. Variations in the transition location strongly affect the surface heat transfer, and can significantly affect the aerodynamics. If suction surface transition does not occur upstream of the throat, there is the likelihood of laminar separation, and consequent significant decrease in blade row aerodynamic efficiency, Murata et al. (1997). Actual turbine blades see a high level of turbulence. And the level of turbulence affects the transition location, as well as the surface heat transfer. Consequently, it is important to determine the effects of turbulence intensity on turbine blade heat transfer and low Reynolds number aerodynamics. The variation in turbulence quantities through a vane passage was studied by Bangert et al. (1997)

While numerous investigators have reported the effects of Reynolds and Mach number variations on turbine blade aerodynamics, the variations in these parameters were relatively small. Typically, the variation was $\pm 50\%$ of the design point value. The turbine vane cascade described herein was designed and built for the purposes of obtaining heat transfer and aerodynamic measurements over a wide range of Reynolds numbers and turbulence intensities. The cascade was connected to a low pressure altitude exhaust system. Measurements were made at inlet total pressures less than 0.2 atm., so that low Reynolds number data were obtained at moderate to transonic Mach numbers. The first item in the test sequence was to obtain aerodynamic measurements for a baseline smooth vane over a range of Reynolds and Mach numbers at different turbulence intensities. It was felt that these data, especially in the low Reynolds number range, could be used to help verify aerodynamic analyses designed to predict the change in blade row efficiency due to variations in Reynolds number, turbulence intensity, and pressure gradients.

The results of an investigation of the effects of Reynolds number and turbulence intensity on overall aerodynamic performance are presented. Since these effects were determined at various exit Mach numbers, the effect of vane surface pressure distribution is also examined. The paper presents the surface pressure distributions and vane loss characteristics as a function of Reynolds and Mach numbers, as well as turbulence intensity. Because these data are intended to help verify aerodynamic analyses, measurements of inlet turbulence length scale are also given. Comparisons are made with results obtained using a Navier-Stokes analysis. The primary purpose of the comparisons was to determine flow conditions where a typical Navier-Stokes analysis using the Baldwin-Lomax (1978) algebraic turbulence model is in good agreement with the data, as well as those regions where it is not.

DESCRIPTION of FACILITY

A plan view of the facility is shown in figure 1. The cascade consists of three vanes and two shaped sidewalls to give four passages. The center vane was the primary test vane. Each of the three vanes had pressure tap instrumentation near midspan. Each sidewall has adjustable tailboards. They were adjusted so that the pressure distribution on each surface of the center vane was the same as the pressure distribution on the corresponding adjacent vane. This gave the same flow in the passages on either side of the test vane. The flow of air was regulated by valves upstream and downstream of the test section. Compressed air was delivered to the test section at a maximum pressure of 207 kPa, (30 psia). Air was exhausted from the test section by an altitude exhaust system capable of maintaining a test section pressure of less than 20 kpa, (3 psia), under low flow conditions. By manipulation of inlet and exit valves the desired Reynolds number and vane row pressure ratio was achieved.

The axial chord was 4.445cm. The true chord-to-axial chord ratio was 2.50. The pitch-to-axial chord ratio was 1.86. The span-to-axial chord ratio was 4.86. This relatively high aspect ratio was chosen to facilitate vane heat transfer measurements. The high aspect ratio assured that the flow was two dimensional in the midspan region. The vane coordinates are given in Table I. The flow turning was approximately 80°. The vane profile is the same as that given by Thulin et al (1982). However, the pitch-to-chord ratio is lower in this cascade. The consequence of the lower pitch-to-chord ratio was to cause the vane pressure distribution to have more diffusion than the original design. The ratio of minimum-to-exit pressure is lower for the tested vane than for the original design. The greater diffusion results in significantly higher losses than for the original design. It is not felt that this is a significant detriment to the tests, since the purposes of the tests were to show relative effects and provide data for comparisons with analyses.

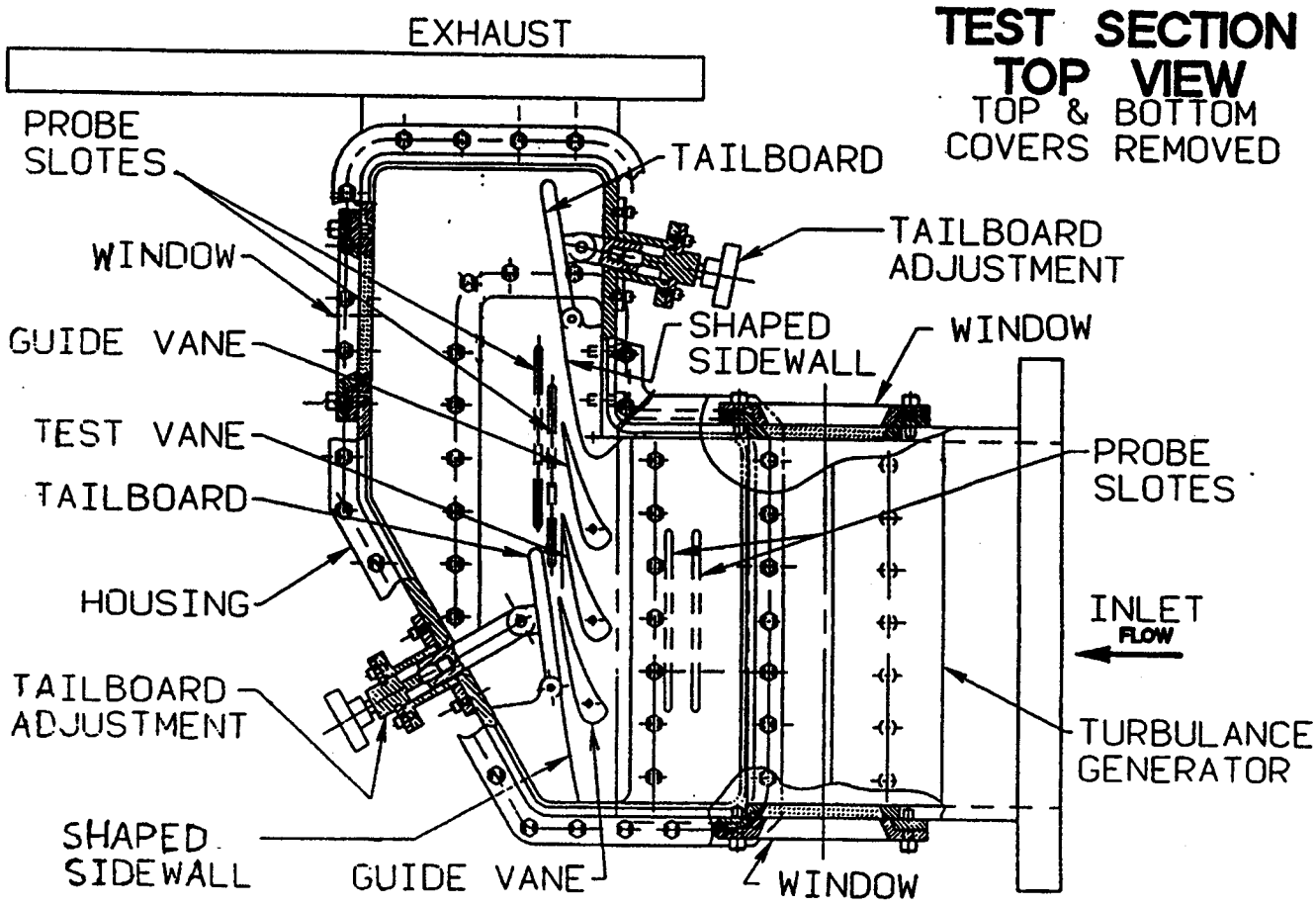

Fig. 1 Overall view of test section.

Four survey slots were installed as part of the test configuration. Two were upstream of the cascade at 1.14 and $2.0c_x$. The other two were downstream of the trailing edge at 0.29 and $0.57c_x$. The window locations shown in figure 1 provided access to verify probe positions. The windows were not used during these tests.

For some tests the turbulence grid shown in figure 2 was installed at $5.71c_x$ in front of the cascade. The design of the grid was based on the one used by O'Brien and Van Fossen (1985). The grid consisted of seven parallel tubes aligned in the spanwise direction. Each tube was 1.59cm in diameter, or $0.36c_x$. Each tube had eight evenly spaced holes. The hole-to-tube diameter ratio was 0.096. High pressure air at up to 900 kpa, (130psia), could be blown through the grid. The grid was reversible so that air could be directed either upstream or in the streamwise direction. Hot wire surveys were conducted in the slots corresponding to 10.4 and 12.8 tube diameters downstream of the grid.

INSTRUMENTATION

Instrumentation consisted of surface static pressures, total pressure and angle surveys, hot wire surveys, and a total temperature measurement upstream of the cascade. The center vane had 24 pressure taps near midspan. In addition to a base pressure measurement, there were 13 suction surface taps, and 10 pressure surface taps. Adjacent vanes were instrumented with either 14 or 10 taps, to give two identically instrumented passages. Two rows, each with 13 endwall static taps spaced one-quarter of a pitch apart, were located at $x/c_x = 1.14$ upstream, and at $x/c_x = 0.35$ downstream of the vane. Each row has 13 static taps spaced one-quarter of a pitch apart. The center upstream tap was on the cascade centerline, and the center downstream tap was on the projection of the center vane camber line. All surface pressures, and some probe pressures

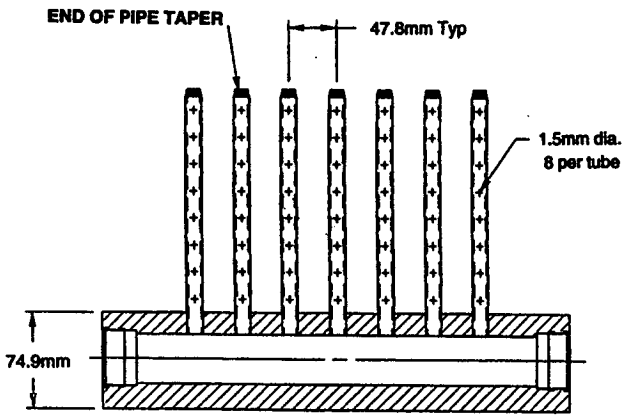

Fig. 2 Turbulence generator.

Table I Vane coordinates

L.E. radius, $r/c_x = 0.15306$ centered at $x/c_x = 0.15306$ $y/c_x = 2.28977$	
Upper surface	
x/c_x 0.5in	y/c_x
0.03581	2.38816
0.10227	2.46023
0.30255	2.54830
0.42614	2.49716
0.55966	2.29546
0.66619	1.93892
0.75000	1.53693
0.91051	0.60795
0.97869	0.17046
1.00242	0.00421
T.E. radius, r/c_x= 0.01866 centered at $x/c_x = 0.98394$ $y/c_x = 0.00161$	
Lower surface	
x/c_x	y/c_x
0.03581	2.19139
0.17046	2.01989
0.25284	1.88210
0.43892	1.51421
0.68324	0.90767
0.78693	0.59375
0.87500	0.30540
0.96619	-0.00415

were measured using a PSI 8400 measuring system. Depending on the desired pressure range, either 34.5 or 103.4 kPa, (5 or 15 psi) transducers were used. Maximum accuracy was achieved by utilizing the fact that individual outputs were the differential pressure from a reference pressure. Thus, a 103.4 kPa, (15 psi), transducer measured pressures between 34.5 and 241.3 kPa, (5 and 35 psia), when the reference pressure was set at 137.9kPa, (20 psia).

Multiple hole pressure probes were used for pitchwise and spanwise surveys in each of the four survey slots. For improved accuracy, cascade total pressure loss was generally measured with a differential pressure transducer. A capacitance differential transducer, (Setra Model 239) was used in parallel with a strain gage differential transducer (SENSOTEC Model 7/43603)) to increase confidence in the measurements. Transducer range was determined by the flow conditions. The range of the transducer was from 1.72 to 17.2 kPa, (0.25 psia to 2.5 psia). At high dynamic pressures, the total pressure loss was measured using the difference in total pressures measured using the PSI system.

Reference total temperature and pressure were measured using two probes. Each was installed near the blade row inlet midway between the vane. The probes were inserted far enough to be outside the endwall boundary layer, but well below the cascade centerline. An additional reference total pressure probe was installed upstream of the turbulence grid. The reference pressures were measured using the PSI system. The total temperature was measured using a type E thermocouple probe.

Hot wire measurements were made in the two survey slots upstream of the cascade using a single wire probe. Turbulence intensity, Tu, and length scale, Λ_x, were measured using a TSI 1211-T1.5 hot wire probe connected to a DANTEC type 55M01 hot wire anemometer. A Concurrent 6350 series computer was used to digitize and analyze the hot wire signal. A 12-bit digitizer was used. The length scale was determined from 2.4 seconds of data, sampled at a rate of 100kHz. Prior to digitization the hot wire signal was filtered at 50kHz using an 8-pole-6-zero, constant delay filter.

Initially, the hot wire was calibrated in an air jet to determine the output voltage, V, as a function of ρU. However, it was later found that measurements, especially of length scale, were more consistent when the hot wire was calibrated in the test facility. In the test facility the calibration duplicated both the dynamic pressure and Reynolds number of the test conditions. Thus, both Reynolds and Grashof numbers were matched during the calibration. The turbulence intensity was calculated using the procedure of Van Fossen et al. (1994).

$$Tu = \frac{d(\rho U)}{dV} \frac{V_{\mathrm{RMS}}}{\rho U}$$

V_{RMS} was measured using an RMS voltmeter with an adjustable time constant. The temperature difference between the time of calibration and run time was small. The hot wire overheat ratio was maintained constant between calibration and test. An analysis showed that small variations in temperature would give a negligible effect on the calibration.

The length scale was calculated using the method of Van Fossen et al. (1994). The length scale was calculated as the average of 58 individual length scales. Each length scale was determined from the autocorrelation of 4096 data points. A least squares fit to an exponential function was used to determine C_τ. Thus:

$$R(\tau) = e^{C_\tau \tau}$$

The average length scale for 58 readings was determined from:

$$\Lambda_x = \frac{1}{58}\sum_{n=1}^{58} U \int_0^\infty R(\tau)d\tau = \frac{1}{58}\sum_{n=1}^{58}\frac{U}{C_\tau}$$

Measurement uncertainty. Measurement accuracy was primarily determined by the accuracy of the pressure measurements. Even though varying the Reynolds number by a factor of ten corresponded to varying the dynamic pressure by nearly a factor of a hundred, it is felt that the velocities were measured to within ±5%. Obtaining accurate velocities over a large range of dynamic pressures was facilitated by using different transducers, each with the appropriate range. An uncertainty analysis was done using the method of Kline and McClintock (1953). In addition, the velocity measurement accuracy was verified by comparing pressure coefficients at different dynamic pressures, but at a constant Reynolds number. This was done at low Mach numbers where the velocity uncertainty was greatest. At low Mach numbers the flow is incompressible, and results should not be affected by Mach number. When the dynamic pressure was varied at constant Reynolds number, the velocities were consistent within ±5%.

An analysis regarding measuring losses showed that the expected uncertainty in the loss coefficient, Y, was approximately ±0.005. It was expected that changes in loss would be consistent to a level better than this value. By using appropriate range transducers the uncertainty in the loss coefficient was minimized.

As pointed out out by Yavuzkurt (1984) the principal uncertainty in the measurement of turbulence intensity is the uncertainty in velocity. Since many of the inlet turbulence intensity measurements occurred at low dynamic pressure, the uncertainty in turbulence intensity at the lowest Reynolds number and high Tu level was estimated to be less than ±10% of the measured value. At Tu = 15%, the absolute uncertainty in Tu was estimated to be less than 1.5%. Again, changes in Tu were expected to be more accurate than this. At turbulence intensities close to 1%, the uncertainty in Tu was estimated to be somewhat larger, but still less than 15% of the measured value. Using the method of Yavuzkurt (1984), the uncertainty in length scale was estimated to be ±10%.

DESCRIPTION of ANALYSIS

A two-dimensional Navier-Stokes analysis was done for selected cases. The code used was the quasi-three dimensional code RVCQ3D. This code has been documented by Chima (1987), and Chima and Yokota (1988). C-type grids are used. They were generated using the method described by Arnone et al. (1992). The approach used to assure accuracy of the calculations was described by Boyle (1991) and by Boyle and Ameri(1997). Results were obtained with different grids to assure that the pressure distributions, and especially the vane row loss, were converged. Neither refining the grid further nor additional iterations gave significantly different pressure distributions or loss levels. The Baldwin-Lomax (1978) turbulence model with Mayle's (1991) transition start criteria was used.

It was not expected that the analysis would give good agreement with the experimental results for all cases. The analytic results are presented primarily to identify those flow conditions where a conventional analysis fails to give good agreement with the experimental data. In this way possible shortcomings, such as in transition modeling, can be identified.

DISCUSSION of RESULTS

Test conditions. Data were obtained for a variety of test conditions. Table II summarizes parameters for the nominal test conditions. The Reynolds numbers given in Table II are based on true chord. Variations in Reynolds number at constant Mach number were achieved by varying the inlet total pressure, P'_{IN}. The variation in turbulence intensity was achieved by using the bar grid. The level of turbulence intensity without the grid was less than 1%. Since the ratio of suction surface length-to-true chord, s_S/c, was 1.26, Reynolds numbers based on suction surface length were 1.26 times greater than those in the Table II. The pressure surface length-to-true chord ratio, s_P/c, was 1.01.

Surface Pressures. The pressure distributions at different exit Mach numbers are given in figures 3 and 4.

Table II Test Conditions

P'_{IN} kPa,(psia)	M_2	Re_2 $\times 10^{-6}$	Tu %
34.5,(5)	0.9	0.55	0.8-12.0
137.9,(20)	0.9	2.21	0.8-12.0
206.8,(30)	0.9	3.31	0.8-12.0
34.5,(5)	0.7	0.49	0.0-12.0
137.9,(20)	0.7	1.95	0.8-12.0
206.8,(30)	0.7	2.92	0.8-12.0
20.7,(3)	0.3	0.148	0.8-12.0
34.5,(5)	0.3	0.247	0.8-12.0
137.9,(20)	0.3	0.988	0.8-12.0
206.8 (30)	0.3	1.481	0.8-12.0

Results for the low Tu cases, with no turbulence grid in place are shown in figure 3. For each value of M_2 results are shown for different values of the exit Reynolds number, Re_2. The surface pressure coefficient, C_p is:

$$C_p = (P'_1 - P)/(P'_1 - P_2)$$

P_2 is the average exit static pressure as measured by the endwall taps. Since the pressure distribution is expressed in terms of C_p, changes in M_2 also change the pressure distribution. The gradient of C_p is proportional to λ, but the proportionality varies with Mach number due to compressibility effects. Symbols denote experimental data, and the curves are from the Navier-Stokes analysis. The pressure distribution corresponds to a vane with "forward loading". The loading distribution is similar to the loadings of the C3X and Mark II vanes as reported by Hylton et al.(1983). There are similarities in the experimental data at all three exit Mach numbers. At each exit Mach number the peak suction surface C_p, or maximum isentropic surface velocity, occurs at or near the highest Reynolds number. The change in peak C_p is not uniform with Reynolds number. While the change is substantial, most of the change in peak C_p occurs over only a fraction of the Reynolds number range. The location of the peak C_p value moved from about 25% of the surface distance to nearly 40% of the suction surface as the Mach number increased. The largest suction surface C_p value occurs at the intermediate Mach number of 0.7. From midway along the suction surface to near the trailing edge, there is little variation in C_p with Reynolds number. A change in C_p from 1.4 to 1.0 corresponds to nearly a 20% decrease in isentropic surface velocity. Thus, all cases show a significant amount of diffusion, and the diffusion increases with Reynolds number. This leads to the expectation of increased boundary layer growth, or separated flow region, with Reynolds number.

Only in the last 25% of the pressure surface distance is there an observed Reynolds number effect. For the two lower Mach numbers the C_p in this region varied in a similar manner to the variation of the suction surface peak C_p. At $M_2 = 0.9$ the variation with Reynolds number was much smaller.

Overall, the analysis correctly predicts the trends in suction surface pressure distribution, and agrees well with the data for the pressure surface. The peak in the suction surface C_p at the lowest Reynolds number is underpredicted at all three exit Mach numbers. The poorest agreement between the analysis and the data occurred for the test condition of lowest Reynolds number and highest Mach number. At this condition the analysis overpredicts C_p midway on the vane suction surface. However, at the next higher Reynolds number the analysis agrees reasonably well with the data. In the analysis, even though there was significant diffusion for the lowest Reynolds number case at $M_2 = 0.9$, the combination of low Re_θ and Tu did not cause the start of transition criteria to be satisfied. The flow went from laminar to fully turbulent when a negative surface shear was calculated, However, it appears that the analysis did not accurately predict the boundary layer behavior in the diffusing flow region at the lowest Reynolds number. The disagreement with the data for this case implies that the suction surface either transitioned, or more likely, had a larger than predicted separation bubble. Of the cases shown, the low Reynolds number at $M_2 = 0.9$ prediction would benefit most from improved turbulence modeling.

Figure 4 shows the same results as figure 3, but with the turbulence grid in place. These results are for the unblown grid. The pressure distributions with high inlet turbulence are similar to the low inlet turbulence distributions. The experimental variation of peak suction surface C_p with Reynolds number was somewhat less at the high level of turbulence. Otherwise the results are similar.

The degree of agreement between the analysis and the data is nearly the same with or without the grid. The analysis was done for $Tu = 10\%$ at the cascade inlet. It will be shown that the experimental inlet turbulence level with the grid installed was somewhat higher than 10%. A level of 10% was chosen as the upstream value to allow for some decay of turbulence upstream of the leading edge. Additional calculations were made with an inlet $Tu = 15\%$. There was no noticeable difference in the calculated surface pressures or overall loss between the two high turbulence levels. The analysis shows a smaller effect of Reynolds number on peak suction surface C_p than is seen in the data. However, at the minimum Reynolds number and $M_2 = 0.9$ the analysis better agrees with the data for high Tu than it did for the low Tu case in figure 3c. The predicted suction surface transition began earlier than it did for the results shown in figure 3a. This is due to the higher inlet turbulence levels.

Figure 5 shows the effect of blowing air through

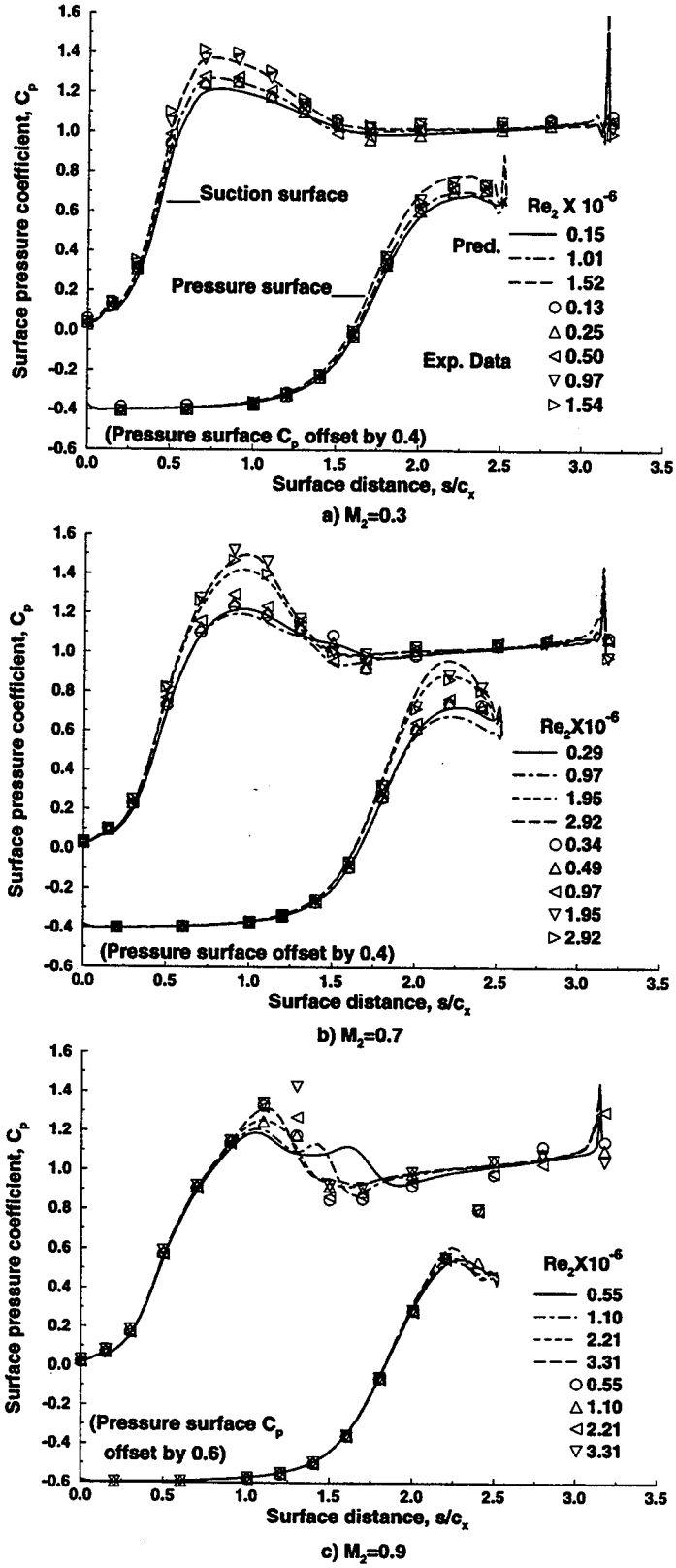

Fig. 3 Surface pressure distribution with no grid.

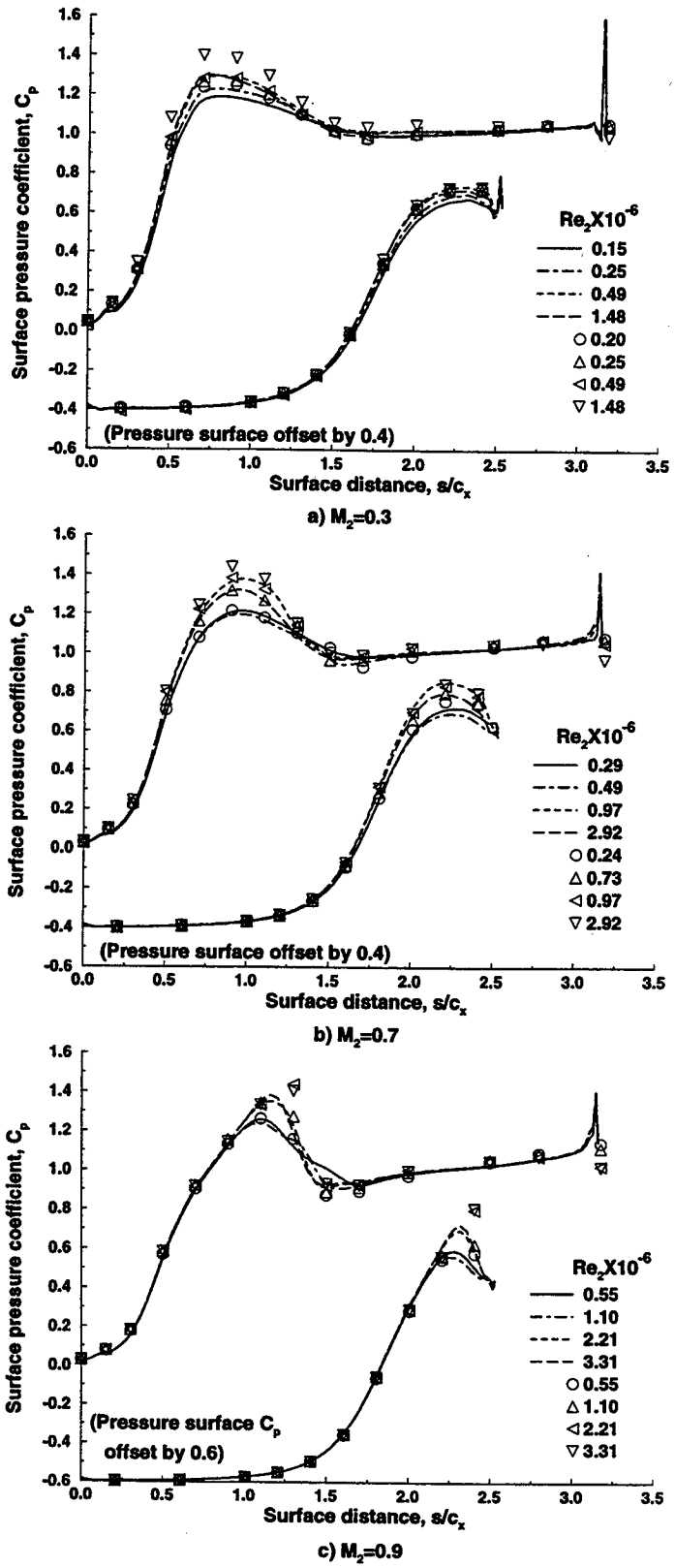

Fig. 4 Surface pressure distribution with grid.

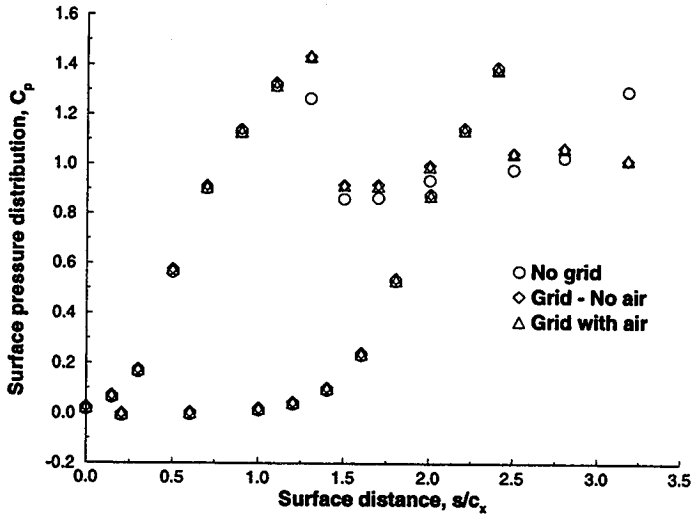

Fig. 5 Effect of grid air on surface pressure distribution, $Re_2 = 1.95 \times 10^6, M_2 = 0.9$

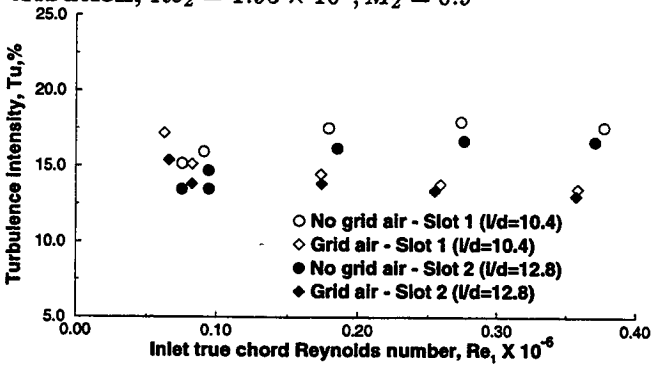

Fig. 6 Average turbulence intensity with grid installed.

the grid on the surface pressure distribution. The turbulence level without the grid was 0.7%. When the grid was in place, the turbulence level was greater than 10% with or without air being blown from the grid. The turbulence levels associated with the grid will be discussed subsequently. There are some differences in the surface pressure distribution between the low turbulence intensity no-grid case and the unblown grid case. However, there are no differences between the blown and unblown grid cases. When air was blown through the grid, it was directed upstream, against the main flow direction. It was found that blowing air upstream against the mainflow direction produced a more uniform turbulence level. When air was blown in the streamwise direction, the turbulence intensity was higher than for the unblown case. However, the pitchwise variation in Tu was much greater than for the unblown case.

Turbulence intensity. Spanwise and pitchwise surveys were made without the grid in place. These surveys showed a uniform Tu of approximately 0.7%, and a corresponding length scale, Λ_x, of 2.0cm. Measurements showed no significant variation in these quantities with Reynolds number.

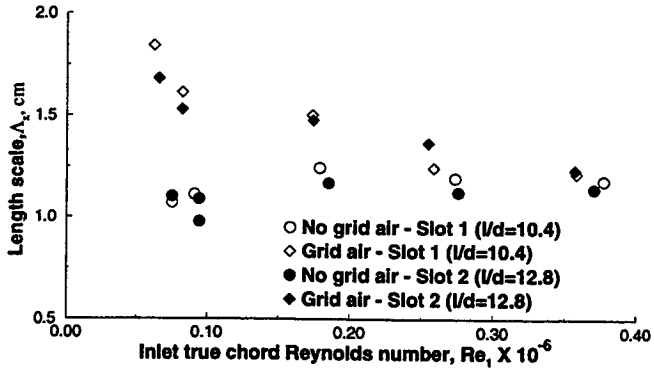

Fig. 7 Average length scale, Λ_x.

Figure 6 shows the pitchwise average turbulence intensity as a function of the inlet Reynolds number with the turbulence grid in place. The inlet Reynolds number was approximately 15% of the exit Reynolds number. Results are shown with and without air being blown out of the grid in the upstream direction. At the highest inlet Reynolds number, the mass flow through the grid was 3.7% of the main flow. Because the air exiting from the grid was choked, the ratio of grid air to mainstream air varied inversely with the inlet Reynolds number. The average turbulence levels are high with the grid in place. The turbulence level is lower for the blown grid. However, as will be shown subsequently, there was a greater degree of pitchwise uniformity for the blown grid. The turbulence intensity is shown for both survey slots. The turbulence decay can be seen, in that the level is lower for the survey further from the grid.

The measured turbulence length scale is shown in figure 7 as a function of inlet Reynolds number. When there was no grid air, increasing the Reynolds number by nearly a factor of five showed little variation in length scale. The average value of approximately 1.1cm is 70% of the diameter of the tubes used to generate turbulence. At the lowest Reynolds number blowing air through the grid increased the length scale by about 60%. However, as the Reynolds number increased the ratio of grid air to mainstream air decreased, and the length scales approached those for no grid air. No length scale growth was observed in moving from slot 1 to slot 2. Young et al. (1992) reported an increase in the length scale by a factor of three for an unblown grid, and by a factor of two for a blown grid, in going from an $l/d = 18$ to an $l/d = 100$. Since the two slots are at l/d of 10.4 and 12.8, a significant increase in length scale was not expected.

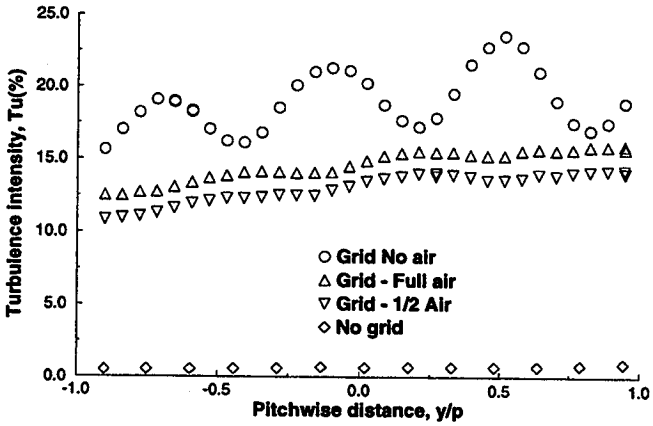

Fig. 8 Turbulence intensity at $x/c_x = 1.14$, $Re_{1c} = 0.37 \times 10^6$

Figure 8 illustrates the degree of uniformity in Tu achieved by the different approaches to generating turbulence. Without air, the grid bar locations are readily apparent. The bar spacing is one-half of the vane pitch. When air is blown in the upstream direction, the signature of the grid bars is not apparent. At this inlet Reynolds number full grid air corresponds to 3.7% of the main flow air. One-half grid air corresponds to half as much air flow from the grid. There is a continuous increase in Tu in the pitchwise direction. The primary cause of this increase is a velocity pitchwise nonuniformity. Inlet pressure surveys and endwall static pressure measurements showed higher velocities in regions of low Tu. The velocity nonuniformity was caused by having only three vanes. Velocities could be made more uniform by adjusting the tailboards. However, moving the tailboards to improve inlet velocity uniformity caused a loss in periodicity for the two passages adjacent to the center vane. The choice was made to maintain periodicity, and tolerate the inlet velocity nonuniformity. Calculations which accounted for the skewing of the inlet velocity showed very little difference from the unskewed calculations.

The length scale, Λ_x, was measured at different pitchwise locations. The variation of Λ_x with pitchwise location, even for the unblown grid, was small.

Vane row efficiency. Total pressure surveys were made in both survey slots downstream of the cascade. Surveys made in the slot nearest the cascade provided the best accuracy. Because of the high turning vane, flow that travels only $0.29c_x$ in the axial direction, travels over one axial chord in the streamwise direction. However, when a probe passes close to the vane trailing edge during a survey, it can modify the static pressure distribution on the vane. This, in turn, can distort the vane row loss measurements. It was found that the interference issue was most significant at the higher Mach

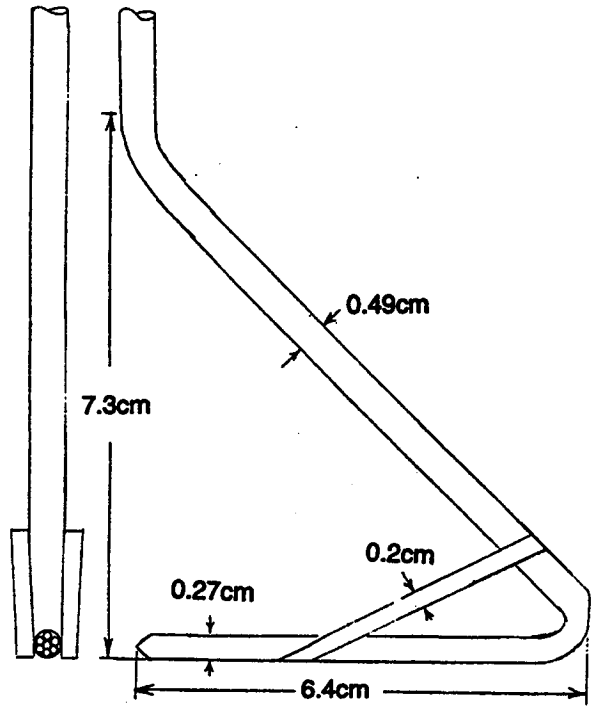

Fig. 9 Schematic of probe used for total pressure surveys.

numbers. Tests were done with a number of total pressure probes. Minimum interference was seen when the stem of the probe was not close to the trailing edge. The surface pressures were less sensitive to the diameter of the probe sensing head than to the probe stem being close to the trailing edge.

The probe used for the measurements is shown in figure 9 . It is a seven-hole probe which can be used for total pressure, flow angle, and static pressure measurements. The main body of the probe is 0.49cm in diameter. At 7.3cm from the bottom the probe is bent at approximately 40 deg. In the measurement plane the stem of the probe is 6.4cm behind the conical head. For the horizontal portion of the probe, the seven sensing tubes are contained in an outer tube 0.27cm in diameter. Two short 0.2cm rods stiffen the horizontal portion of the probe.

Loss measurements are shown in figure 10. The losses are shown for three Mach numbers over a range of Reynolds numbers for two turbulence intensities. All of the high turbulence intensity results were obtained with the unblown grid. A number of loss surveys were made with air blown through the grid. There was no evidence of different losses between blowing and not blowing air through the grid. The loss is presented in terms of Y, which is defined as:

$$Y_A = (P_1' - P_2')/(P_1' - P_2)$$

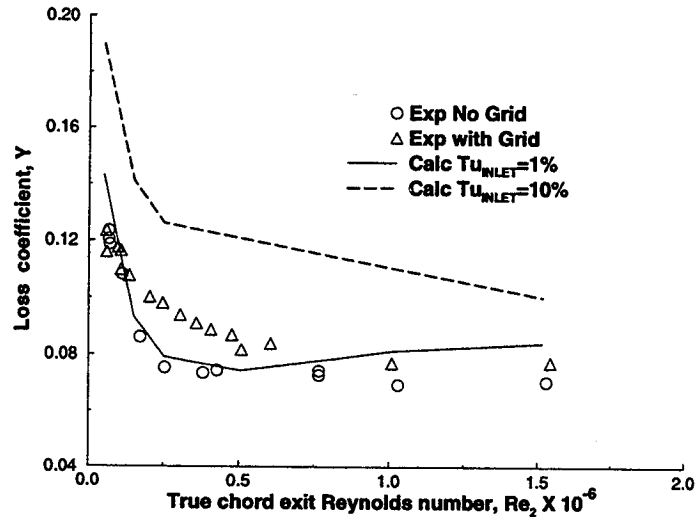

a) M_2=0.3

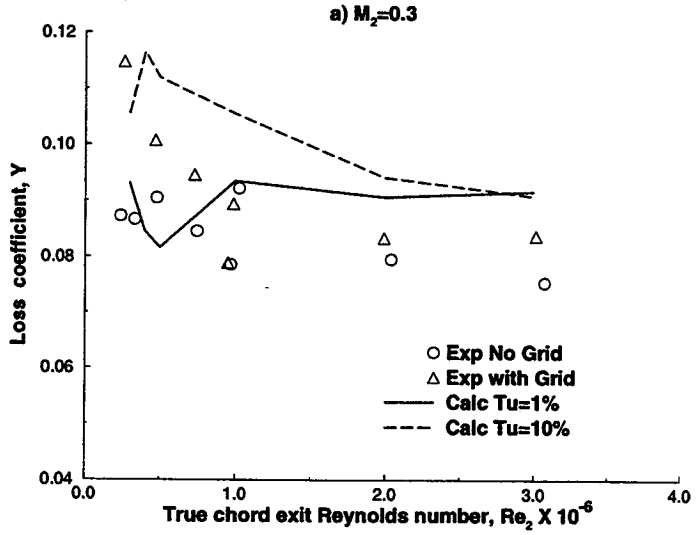

b) M_2=0.7

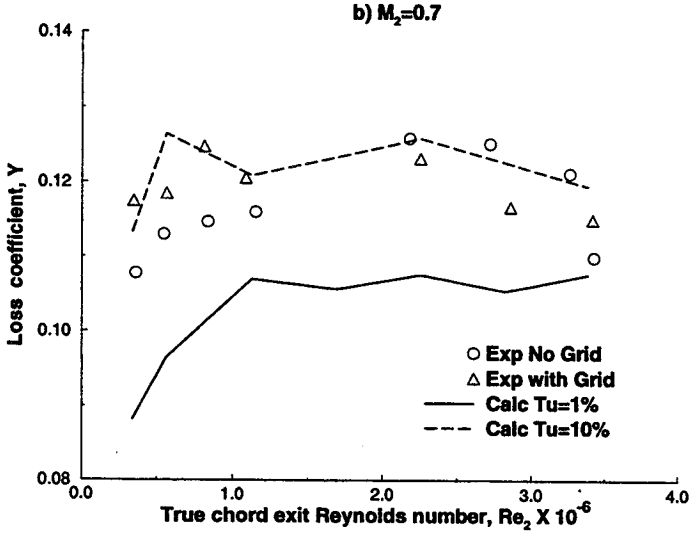

c) M_2=0.9

Fig. 10 Area averaged loss coefficient.

Only area averaged results are shown. Additional calculations were done to determine the mass averaged kinetic energy loss coefficient, $\overline{e}_M$, which is defined as:

$$\overline{e}_M = \frac{\int_{p-0.5}^{p+0.5} \rho_2 cos\alpha V_2 \left[\frac{\left((P_1'/P_2')^{\frac{\gamma}{\gamma-1}}-1\right)}{\left((P_1'/P_2)^{\frac{\gamma}{\gamma-1}}-1\right)}\right]}{\int_{p-0.5}^{p+0.5} \rho_2 cos\alpha V_2}$$

Expressing the loss in terms of a mass averaged $\overline{e}_M$ involved additional uncertainties, principally involving the flow angle, α. Comparing losses calculated using $\overline{e}_M$ and Y_A showed no significant relative changes. Therefore, Y was chosen, since it is a more direct calculation.

Figure 10a shows results for an exit Mach number of 0.3. For Reynolds numbers less than about 300,000 the experimental losses at low turbulence decrease with increasing Reynolds number. Beyond $Re_2 = 300,000$ the loss level remains fairly constant. At a high inlet turbulence intensity the loss levels at low Reynolds numbers generally exceed the low inlet turbulence intensity losses. At the minimum Reynolds number the loss levels with or without the grid are nearly the same. It appears that at low Reynolds numbers and low turbulence intensity a separation bubble forms, which may not close. This, in turn, leads to large momentum deficits. The high turbulence intensity causes more rapid boundary layer growth, but may also decrease the degree of suction surface separation. It is sometimes assumed, Japikse and Baines(1994), that losses should decrease with Reynolds number, even in the turbulent flow regime. The reason that this vane does not show this behavior is because of the increased suction surface diffusion with increased Reynolds number as was seen in figures 3 and 4.

The analysis is in reasonably good agreement with the data for the low turbulence intensity results. However, the analysis overpredicts the loss level at high turbulence. The combination of good agreement for low turbulence, when laminar flow prevails, and poor agreement at high turbulence indicates that the Baldwin Lomax (1978) turbulence model may not accurately predict losses.

The results in figure 10b for an exit Mach number of 0.7 are somewhat similar to those in figure 10a. One noticeable difference is that the low turbulence intensity data show losses only slightly affected by Reynolds number. It may be that, at the higher Mach number, measurements were taken at Reynolds numbers too high to show the same upturn in loss seen in figure 10a. The minimum Reynolds number nearly doubled when the exit Mach number increased from 0.3 to 0.7. Except at the lowest Reynolds number the predicted high Tu losses are greater than the measured loss. At low Reynolds numbers the low Tu prediction agrees well with the low Tu measurements. At high Reynolds numbers, the predicted loss level for both Tu levels are very close to each other. In this region the predictions are somewhat higher than the experimental data.

The experimental results shown in figure 10c for an exit Mach number of 0.9 show a different behavior than for the other two Mach numbers. At both turbulence intensities, losses initially increase with increasing Reynolds number. This is consistent with the pressure distributions shown in figures 3 and 4, which showed that the maximum C_p increased with increasing Reynolds number. The increased diffusion apparently contributed to higher loss levels. The higher C_p also leads to the expectation that shock losses increased as Reynolds number increased. A $C_p = 1.5$ corresponds to an isentropic surface Mach number of 1.25 with $M_2 = 0.9$

The degree of agreement between the analysis and the experimental data is different at $M_2 = 0.9$ than for the two lower Mach numbers. The low turbulence intensity results are underpredicted by the low Tu analysis. Except at low Reynolds numbers, both the low and high turbulence intensity results are reasonably well predicted by the high Tu analysis. The comparisons between the results for $M_2 = 0.3$ and $M_2 = 0.9$ are not inconsistent. The change in predicted Y between low and high turbulence intensity cases is nearly the same for both Mach numbers. If the low Tu analysis had correctly predicted losses for $M_2 = 0.9$, then the high Tu analysis probably would overpredict the losses for the grid data as much as it overpredicted the data for $M_2 = 0.3$.

At all three Mach numbers the magnitude of the loss, Y, was larger than might be expected for turbine vanes. The high flow turning of approximately 80°, along with the high solidity resulting from a true chord-to-pitch ratio of 1.34 are the primary causes for the high loss levels.

CONCLUSIONS

The work showed the variation in surface pressures, and losses for large variations in Reynolds and Mach numbers, as well as turbulence intensity for a turbine vane characterized by "forward loading". For the particular vane tested the effect of high freestream turbulence was to increase the loss level, Y. Only at the minimum Reynolds number were the loss levels equal at both high and low turbulence levels. At higher Reynolds numbers, losses were greater, though not substantially so, when there was a high turbulence level.

At each exit Mach number the peak C_p increased significantly with increasing Reynolds number. Despite the increased diffusion that this represents, losses at $M_2 = 0.3$ initially decreased with increased Reynolds number for both turbulence intensity levels. The loss levels at $M_2 = 0.7$ initially decreased only for the high turbulence intensity. The data at low Tu did not significantly vary with Reynolds number. At high Reynolds numbers for all Mach numbers, and for all Reynolds numbers at $M_2 = 0.9$, the loss level was relatively independent of Reynolds number for both levels of turbulence intensity. The increase in suction surface diffusion with increased Reynolds number is felt to be the cause for this behavior.

With the grid in place, high turbulence levels were achieved upstream of the vane. When there was no air from the grid, there was a noticeable nonuniformity in the turbulence level. The turbulence intensity was highest in the wake of the grid. Blowing air at very high velocities in the upstream direction resulted in a more uniform turbulence level in front of the vane. While high turbulence levels were found when the grid air was in the streamwise direction, the turbulence level was very nonuniform.

Predictions of the vane performance using a two-dimensional Navier-Stokes analysis showed good agreement for the surface pressure distributions at both levels of turbulence. The analysis showed less variation in suction surface peak C_p with Reynolds number than was measured. Otherwise, the agreement was good. The analysis showed a higher increment in loss than was shown by the data, when the inlet turbulence level increased. Because the loss level was correctly predicted for the low turbulence cases when the flow was entirely subsonic, the applicability of the Baldwin-Lomax turbulence model for loss predictions seems questionable. The loss predictions agreed with the data when the flow was more likely to be laminar, and shock free. In summary, it is hoped that these data will be useful for researchers to verify new approaches to predicting turbine blade aerodynamic performance.

REFERENCES

Arnone, A., Liou, M.-S., and Povinelli, L. A., 1992, "Navier- Stokes Solution of Transonic Cascade Flows Using Non-Periodic C-Type Grids," AIAA *Journal of Propulsion and Power,* Vol. 8, No. 2, pp. 410-417.

Baldwin, B.S. and Lomax, H., 1978, "Thin-Layer Approximation and Algebraic Model for Separated Turbulent Flows," AIAA paper AIAA-78-257.

Bangert, B.A., Kohli, A., Sauer, J.H., and Thole, K.A., 1997, "High Freestream Turbulence Simulation in a Scaled-Up Turbine Vane Passage," ASME paper 97-GT-51

Boyle, R.J., 1991, "Navier-Stokes Analysis of Turbine Blade Heat Transfer," ASME *Journal of Turbomachinery,* Vol. 113, pp. 392-403.

Boyle, R.J., and Ameri, A..A., 1997, "Grid Orthogonality Effects on Predicted Turbine Midspan Heat Transfer and Performance," ASME *Journal of Turbomachinery,* Vol. 119, pp. 31-38.

Chima, R.V., 1987, "Explicit Multigrid Algorithm for Quasi-Three- Dimensional Flows in Turbomachinery," AIAA *Journal of Propulsion and Power,* Vol. 3, No. 5, pp. 397-405.

Chima, R.V., and Yokota, J.W., 1988, "Numerical Analysis of Three-Dimensional Viscous Internal Flows," AIAA paper AIAA 88-3522, (NASA TM-100878).

Hourmouziadis, J., 1989, "Aerodynamic Design of Low Pressure Turbines," AGARD Lecture Series, No 167.

Hylton, L.D., Mihelc, M.S., Turner, E.R., Nealy, D.A., and York, R.F., 1983, "Analytical and Experimental Evaluation of the Heat Transfer Distribution Over the Surfaces of Turbine Vanes," NASA CR-168015.

Japikse, D., and Baines, N.C., 1994, "Introduction to Turbomachinery", Concepts ETI, Norwich, and Oxford Univ. Press Oxford, publishers.

Kline, S.J., McClintock, F.A., 1953, "Describing Uncertainties in Single-Sample Experiments," *Mechanical Engineering,* Vol. 75, pp 3-8.

Mayle, R.E., 1991, "The Role of Laminar-Turbulent Transition in Gas Turbine Engines," ASME *Journal of Turbomachinery,* Vol. 113, pp. 509-537.

Murata, K., Abe, H., and Tsutsui, Y., 1997, "Characteristics of a Turbine Cascade at Low Reynolds Numbers," ASME paper 97-GT-54.

O'Brien, J.E., and Van Fossen, G.J., 1985, "The Influence of Jet-Grid Turbulence on Heat Transfer From the Stagnation Region of a Cylinder in Crossflow," NASA TM-87011.

Thulin, R.D., Howe, D.C., and Singer, I.D., 1982, "Energy Efficient High-Pressure Turbine Detailed Design Report," NASA CR-165608.

Van Fossen, G.J., Simoneau, R.J., and Ching, C.Y., 1994, "Influence of Turbulence Parameters, Reynolds Number, and Body Shape on Stagnation-Region Heat Transfer," NASA TP-3487

Yavuzkurt S., 1984, "A Guide to Uncertainty Analysis of Hot-Wire Data," ASME *Journal of Fluids Engineering,* Vol. 106, pp. 181-186.

Young, C.D., Han, J.C., Huang, Y., and River, R.B., 1992, "Influence of Jet-Grid Turbulence on Flat Plate Turbulent Boundary Layer Flow and Heat Transfer," ASME *Journal of Heat Transfer,* Vol. 114, pp. 65-72.

REPORT DOCUMENTATION PAGE

Form Approved
OMB No. 0704-0188

1. AGENCY USE ONLY (*Leave blank*)	2. REPORT DATE	3. REPORT TYPE AND DATES COVERED
	June 1998	Technical Memorandum

4. TITLE AND SUBTITLE

Aerodynamics of a Transitioning Turbine Stator Over a Range of Reynolds Numbers

5. FUNDING NUMBERS

WU–523–26–13–00

6. AUTHOR(S)

R.J. Boyle, B.L. Lucci, V.G. Verhoff, W.P. Camperchioli, and H. La

7. PERFORMING ORGANIZATION NAME(S) AND ADDRESS(ES)

National Aeronautics and Space Administration
Lewis Research Center
Cleveland, Ohio 44135–3191

8. PERFORMING ORGANIZATION REPORT NUMBER

E–11243

9. SPONSORING/MONITORING AGENCY NAME(S) AND ADDRESS(ES)

National Aeronautics and Space Administration
Washington, DC 20546–0001

10. SPONSORING/MONITORING AGENCY REPORT NUMBER

NASA TM—1998-208408
98–GT–285

11. SUPPLEMENTARY NOTES

Responsible person, R.J. Boyle, organization code 5820, (216) 433–5889.

12a. DISTRIBUTION/AVAILABILITY STATEMENT

Unclassified - Unlimited
Subject Category: 34 Distribution: Nonstandard

This publication is available from the NASA Center for AeroSpace Information, (301) 621–0390.

12b. DISTRIBUTION CODE

13. ABSTRACT ***(Maximum 200 words)***

Midspan aerodynamic measurements for a three vane-four passage linear turbine vane cascade are given. The vane axial chord was 4.45 cm. Surface pressures and loss coefficients were measured at exit Mach numbers of 0.3, 0.7, and 0.9. Reynolds number was varied by a factor of six at the two highest Mach numbers, and by a factor of ten at the lowest Mach number. Measurements were made with and without a turbulence grid. Inlet turbulence intensities were less than 1% and greater than 10%. Length scales were also measured. Pressurized air fed the test section, and exited to a low pressure exhaust system. Maximum inlet pressure was two atmospheres. The minimum inlet pressure for an exit Mach number of 0.9 was one-third of an atmosphere, and at a Mach number of 0.3, the minimum pressure was half this value. The purpose of the test was to provide data for verification of turbine vane aerodynamic analyses, especially at low Reynolds numbers. Predictions obtained using a Navier-Stokes analysis with an algebraic turbulence model are also given.

14. SUBJECT TERMS

Turbine; Aerodynamics

15. NUMBER OF PAGES

18

16. PRICE CODE

A03

17. SECURITY CLASSIFICATION OF REPORT	18. SECURITY CLASSIFICATION OF THIS PAGE	19. SECURITY CLASSIFICATION OF ABSTRACT	20. LIMITATION OF ABSTRACT
Unclassified	Unclassified	Unclassified	